Microwave- and Thermally-Promoted Iminyl Radical Cyclizations: A Versatile Method for the Synthesis of Functionalized Pyrrolines

*Jatinder Singh, Tanner J. Nelson, Samuel A. Mansfield, Garrison A. Nickel, Yu Cai, Dakota D. Jones, Jeshurun E. Small, Daniel H. Ess, and Steven L. Castle**

Department of Chemistry and Biochemistry, Brigham Young University, Provo, Utah 84602

scastle@chem.byu.edu

TOC Graphic.

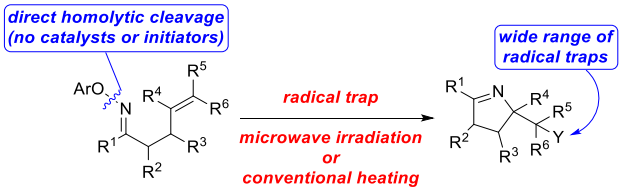

ABSTRACT. A detailed study of iminyl radical cyclizations of *O*-aryloximes tethered to alkenes is reported. The reactions can be triggered by either microwave irradiation or conventional heating in an oil bath. A variety of radical traps can be employed, enabling C–C, C–N, C–O, C–S, or C–X bond formation and producing a diverse array of functionalized pyrrolines. Substrates containing an allylic sulfide furnish terminal alkenes by a tandem cyclization–thiyl radical β-elimination pathway. Cyclizations of hydroxylated substrates exhibit moderate diastereoselectivity that in some cases can partially be attributed to intramolecular hydrogen bonding. Computational studies suggested a possible role for thermodynamics in controlling the stereochemistry of cyclizations. The reaction temperature can be lowered from 120 °C

to 100 °C by employing *O*-(*p*-*tert*-butylphenyl)oximes instead of *O*-phenyloximes as substrates, and these second-generation iminyl radical precursors can be used in a one-pot oxime ether formation–cyclization that is promoted by conventional heating. The functionalized pyrrolines obtained from these reactions can be conveniently transformed in several different ways.

INTRODUCTION

Iminyl radical cyclizations[1] occupy a central role in the growing field of nitrogen-centered radical chemistry.[2] Seminal observations by Forrester[3] were followed by Zard's pioneering work[4] and Weinreb's contributions[5] that rendered these transformations practical. Recently, developments in the areas of photoredox and transition metal catalysis have inspired the discovery of several iminyl radical cyclications that generate functionalized pyrrolines. Many of these processes are initiated by single-electron transfer (SET) reduction of *O*-acyloximes or *O*-aryloximes, producing iminyl radicals that subsequently cyclize onto tethered alkenes. The resulting cyclic radical must then be oxidized to enable catalyst turnover (Scheme 1a). This requirement constrains the type of reagents that can be employed to functionalize the intermediate adduct.[6,7]

Forrester's early studies[3] inspired the development of an oxidative process that is complementary to reductive iminyl radical cyclizations. Studer[8] and Leonori[9] independently demonstrated in 2017 that iminyl radicals can be formed via SET oxidation of α-imino oxy acids and then cyclized to furnish pyrrolines. In this case the cyclic radical adduct is reduced to close the catalytic cycle, thereby allowing a wider range of trapping agents to be employed when compared to the cyclizations initiated by SET reduction (Scheme 1b). A few additional reports of oxidative iminyl radical cyclizations[10] have followed, illustrating the utility of this protocol in the synthesis of pyrrolines. However, the requisite redox cycle still precludes the use of certain traps to functionalize the intermediate cyclic adduct. Moreover, the need to deprotonate the carboxylic acid moiety of the substrate prior to SET oxidation renders base-sensitive trapping agents unsuitable.[8–10] Clearly, the ability to eschew SET processes in the production of iminyl radicals[11] would advance the field by enabling the use of a broad range of traps including those that are

incompatible with redox cycles. Such a development would facilitate the synthesis of a wide range of functionalized pyrrolines, many of which either possess useful biological activity[12] or can be transformed into medicinally important pyrrolidines.[13]

In 1999, Narasaka established that *O*-2,4-dinitrophenyloximes could produce iminyl radicals upon SET reduction of the electron-deficient aromatic ring followed by homolytic cleavage of the N–O bond.[14] Mulder, Ingold, and Walton then reported iminyl radical formation via thermally promoted homolysis of the weak N–O bond present in *O*-phenyloximes (BDE = ca. 35 kcal/mol).[15] Walton leveraged this discovery in 2007 by disclosing that microwave-promoted scission of *O*-phenyloximes facilitates iminyl radical cyclizations that do not require initiators or catalysts and are terminated by hydrogen atom abstraction from the toluene solvent.[16] Inspired by this work, we recognized that employing solvents that are not competent hydrogen atom donors would broaden the scope of these reactions by enabling functionalization rather than reduction of the radical intermediates. Accordingly, we devised a synthesis of 2-acylpyrroles featuring 5-*exo*-*dig* cyclizations of iminyl radicals with $PhCF_3$ as solvent and TEMPO trapping.[17] We later applied microwave-promoted homolysis of *O*-phenyloximes to the construction of functionalized nitriles via fragmentations of cyclic iminyl radicals and trapping of the resulting cyanoalkyl radicals with reagents capable of forging C–C, C–O, C–N, or C–X bonds.[18] These discoveries encouraged us to revisit Walton's microwave-promoted pyrroline synthesis. We reasoned that replacing the toluene solvent with poor hydrogen atom donors such as $PhCF_3$, CH_3CN, or CH_3OH would allow trapping of the cyclic radical intermediate with a wide range of agents, including some that would not be compatible with the redox cycles inherent to most modern iminyl radical cyclizations (Scheme 1c). We recently published a preliminary report demonstrating the viability of microwave-promoted catalyst-free 5-*exo*-*trig* iminyl radical cyclizations for the construction of various functionalized pyrrolines.[19] Herein we provide a comprehensive description of these studies. Notable advances since our initial report include a second-generation iminyl radical precursor that is in many cases more efficient than the original *O*-phenyloxime, thermally-promoted cyclizations with oil bath heating that are convenient for large-scale reactions, a one-

pot oxime ether formation–cyclization process, and a detailed experimental and computational study of the factors underlying the diastereoselective cyclizations of alcohol-containing substrates.

Scheme 1. Comparison of Iminyl Radical Cyclization Methods

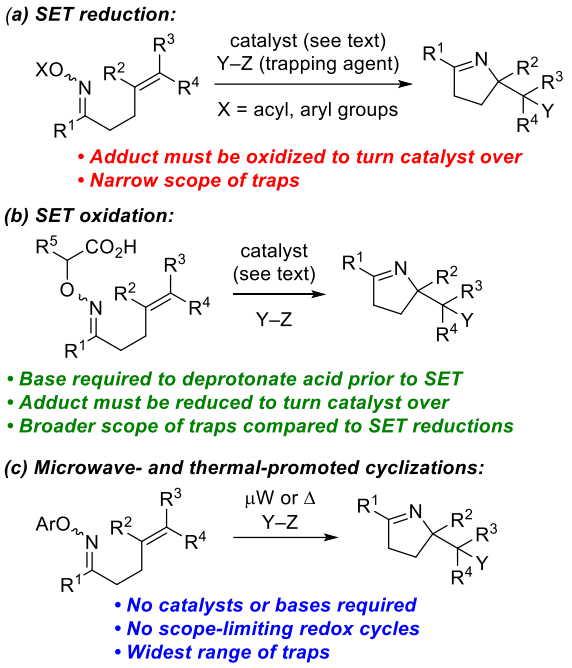

RESULTS AND DISCUSSION

We commenced our investigation by studying the cyclization of *O*-phenyloxime **1** with allylsulfone **2a**[20] as the radical trap (Table 1). The allylsulfone was employed in excess (≥3 equiv), and the ratio of pyrroline adduct **3a** to unreacted **2a** was readily determined by ^{1}H NMR spectroscopy. This simple method of measuring the yield accelerated the optimization process. Our first cyclization was conducted at 100 °C in $PhCF_3$, and a low yield (20%) of **3a** was obtained (entry 1). Increasing the temperature to 120 °C was helpful (entry 2), but a further increase to 130 °C did not improve the yield (entry 3). The polar solvents CH_3OH and CH_3CN were also not beneficial (entries 4 and 5). Ultimately, we found that extending the time of the reaction conducted at 120 °C in $PhCF_3$ from 45 min to 2 h delivered pyrroline **3a** in 72% isolated yield (entry 6). Phenol was detected as a separable byproduct of each reaction, demonstrating that the phenoxy radical generated in the initial homolysis step subsequently participates in adventitious hydrogen atom abstraction. Furthermore, the presence of some dark insoluble material in the reaction mixtures provides indirect evidence that this radical byproduct can also polymerize.

Table 1. Optimization of Reaction Conditions

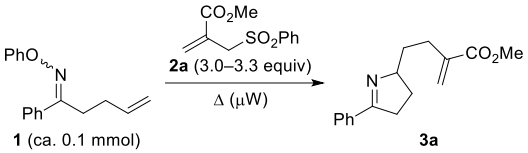

entry	solvent	temp (°C)	time (min)	yield of **3a** (%)
1	$PhCF_3$	100	60	20[a]
2	$PhCF_3$	120	45	35[a]
3	$PhCF_3$	130	45	30[a]
4	CH_3OH	110	45	30[a]
5	CH_3CN	120	120	41[b]
6	$PhCF_3$	120	120	72[b]

[a]Calculated from ^{1}H NMR spectra of reaction mixtures. [b]Isolated yield.

We then applied the optimized conditions to cyclizations of **1** conducted in the presence of various radical traps as shown in Figure 1. We were pleased to discover that most of these reagents facilitated the construction of pyrrolines **3** in good yields. For instance, trapping of the cyclic radical intermediate with TEMPO forged a C–O bond, furnishing pyrroline **3b** in high yield (entry 2). Carbon–halogen bonds could be generated by using CCl_4,[21] CBr_4,[22] or 2-iodopropane[23] as trapping agents (entries 3–5), although the C–I bond formation proceeded in modest yield. Interestingly, bromide **3d** was accompanied by a separable dibrominated adduct that was obtained in ca. 10% yield (vide infra). Sulfonyl azide **2f**[24] and xanthate **2g**[25] were capable of mediating C–N and C–S bond construction, respectively (entries 6 and 7). Finally, the benziodoxolone radical trap **2h**[26] was able to facilitate C–C bond formation by delivering pyrroline **3h** in good yield (entry 8). The compatibility of a wide range of radical traps with these iminyl radical cyclizations can at least partly be attributed to the absence of SET steps and redox cycles.

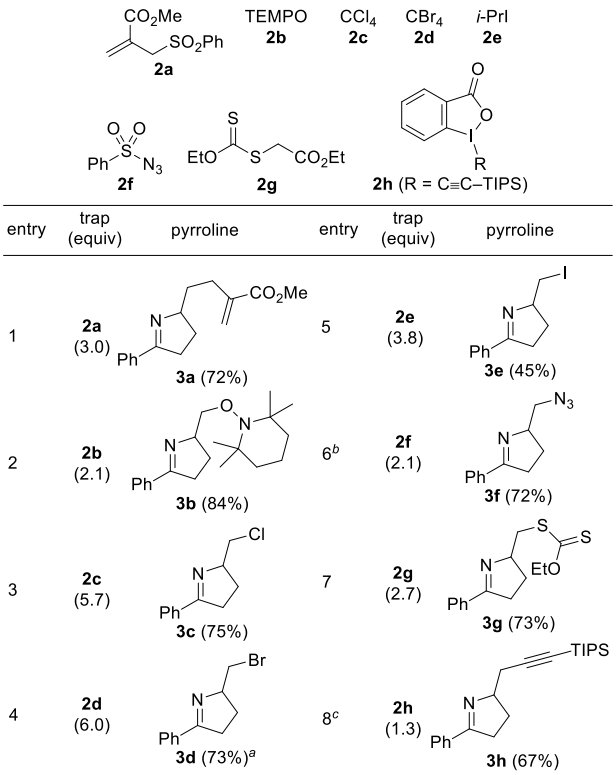

Figure 1. Scope of radical traps in cyclizations of **1** (ca. 0.1 mmol). Conditions were $PhCF_3$, 120 °C (μW), and 1–2 h unless otherwise specified. [a]A dibrominated pyrroline was also obtained in ca. 10% yield. [b]Irradiated at 110 °C for 5 h. [c]Irradiated at 110 °C for 2 h.

Unfortunately, our attempts to forge C–F bonds via this method were unsuccessful. Reactions employing Selectfluor® as the radical trap[21] (Figure 2) provided only trace amounts of the targeted fluorinated pyrroline that could be detected by mass spectrometry but not isolated. The most abundant component of the complex reaction mixture (ca. 10–15%) was an adduct formed by trapping of the cyclic radical intermediate by $PhCF_3$ instead of Selectfluor®. This result indicated that the solvent was able to outcompete the reagent for the intermediate. We hypothesized that the poor solubility of Selectfluor® in $PhCF_3$ was at least partly responsible for this problem. However, reactions performed in solvents that dissolve this bis-ammonium salt (i.e., CH_3CN, CH_3OH) did not produce the desired fluorinated pyrroline. Attempts to employ *N*-fluorobenzenesulfonimide (NFSI) as a radical fluorinating agent[27] (Figure 2) were also futile. Further investigations revealed that microwave irradiation of *O*-phenyloxime **1** in solution without a radical trap present induced slow formation of the aforementioned $PhCF_3$ adduct. Thus, reagents

must be able to react with radicals faster than this solvent to be viable trapping agents in these microwave-promoted cyclizations.

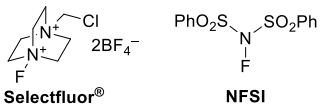

Figure 2. Unsuccessful radical traps.

Allylic sulfides are attractive radical acceptors, as they can participate in a tandem radical cyclization–β-elimination process that incorporates a synthetically useful terminal alkene into the final product.[28] Accordingly, we evaluated *O*-phenyloxime **4**, which contains an allylic sulfide, as a substrate for iminyl radical cyclization (Scheme 2). We were pleased to find that **4** underwent cyclization and subsequent elimination upon microwave irradiation at 120 °C, furnishing pyrroline **5**. Importantly, the thiyl radical that is released in the elimination step did not have any deleterious impacts on the reaction.

Scheme 2. Tandem Cyclization–Radical β-Elimination

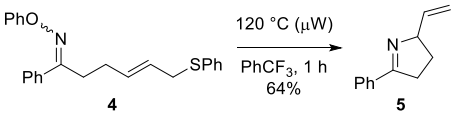

The microwave-promoted iminyl radical cyclizations with TEMPO trapping exhibited a broad scope with respect to the structures of the substrates as outlined in Scheme 3. Each *O*-phenyloxime **6** was constructed via condensation of a known or commercially available ketone with *O*-phenylhydroxylamine hydrochloride ($PhONH_2$•HCl). The presence of an aryl group in conjugation with the oxime ether (e.g., **1**) was not required, as evidenced by the production of alkyl-substituted pyrroline **7a**. The process was not limited to terminal alkenes, as disubstituted (**7b**) and trisubstituted (**7c**) alkene acceptors were tolerated. A cyclic alkene was a viable acceptor, delivering *cis*-fused bicyclic adduct **7d** with high diastereoselectivity due to TEMPO engaging the radical intermediate primarily from its convex face. An α,α-dimethyl-substituted *O*-phenyloxime afforded pyrroline **7e**; this cyclization is noteworthy because it establishes that 5-*exo*-*trig* iminyl radical cyclization can outcompete a fragmentation that would have furnished a nitrile and a tertiary alkyl radical. Interestingly, cyclizations of α- and β-substituted *O*-

phenyloximes yielded results that depended on the identities of the substituents. Whereas cyclizations of methyl-substituted *O*-phenyloximes produced pyrrolines **7f** and **7h** with low diastereoselectivity (1.4:1 and 2.4:1 dr, respectively), cyclizations of the analogous hydroxy-containing substrates yielded pyrrolines **7g** and **7i** with higher selectivity (2.6:1 and 4.2:1 dr,[29] respectively). In addition, the major isomers of β-substituted pyrrolines **7h** and **7i** were of opposite relative stereochemistry. Unfortunately, the inseparable nature of the diastereomers of **7f** combined with their overlapping spectral signals precluded the assignment of their relative stereochemistry. The yields of alcohols **7g** and **7i** were lower than those of their methyl congeners **7f** and **7h**. We suspect that the hydroxy-substituted pyrrolines can degrade either in the course of purification or during the reaction due to hydrogen atom abstraction by various endogenous radicals. However, we have been unable to isolate or characterize any byproducts that would support this hypothesis.

Scheme 3. Scope of *O*-Phenyloxime Substrates

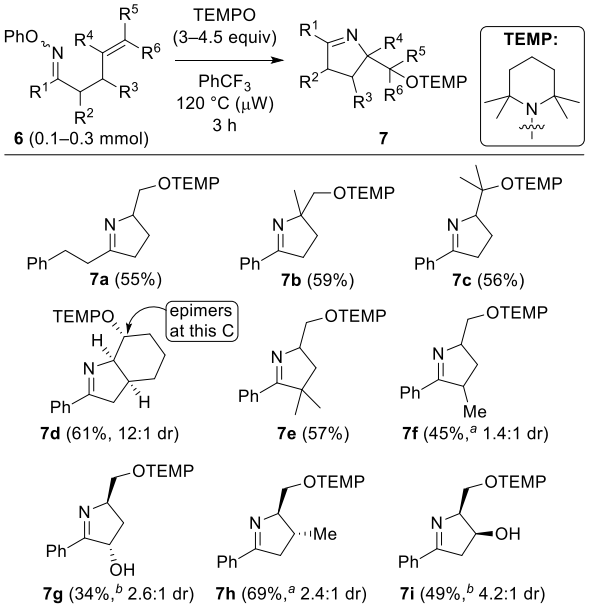

[a]Combined isolated yield of both diastereomers. [b]Isolated yield of major diastereomer.

We posited that the ability of hydroxy-substituted substrates and intermediates to form intramolecular hydrogen bonds could be the origin of the contrasting stereochemical results. To probe this idea, we performed cyclizations of β-hydroxy-substituted *O*-phenyloxime **6i** in various polar solvents that would

presumably disrupt intramolecular hydrogen bonding. Reactions conducted in DMF, CH_3OH, and CH_3CN were all characterized by attenuated diastereoselectivity (Table 2). Additionally, the yields of these reactions varied widely, demonstrating the profound impact of solvent on this process. Interestingly, cyclization of β-methoxy-substituted *O*-phenyloxime **8** exhibited inverted stereoselectivity, furnishing *trans*-substituted pyrroline **9** as the major product (Scheme 4). These observations provide compelling evidence for the importance of an intramolecular hydrogen bond as an element of stereocontrol in the cyclization of **6i**.

Table 2. Cyclizations of 6i in Various Solvents

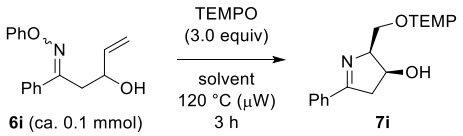

entry	solvent	yield (%)[a]	dr[b]
1	$PhCF_3$	49	4.2:1
2	DMF	71	1.2:1
3	CH_3OH	4	1.7:1
4	CH_3CN	21	1.1:1

[a]Isolated yield of major diastereomer. [b]Calculated from ^{1}H NMR spectra of reaction mixtures.

Scheme 4. Cyclization of β-OMe-Substituted *O*-Phenyloxime

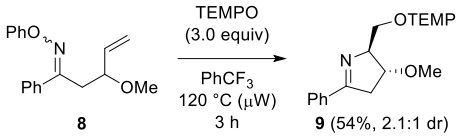

DFT calculations (Gaussian 16)[30] performed at the UM06-2X/6-311++G** level of theory[31] were used to examine possible intramolecular hydrogen bonding during the cyclization of **6i**. Figure 3a shows the two lowest-energy optimized transition-state structures for the iminyl radical C–N bond-forming step. These structures were located by sampling conformational space using x-TB/CREST[32] followed by full M06-2X optimization of several low-energy conformers. Energies and structural optimization included the PCM[33] solvent model for $PhCF_3$. Minima and transition-state structures were verified through

vibrational frequency analysis. Enthalpies of the lowest energy transition state conformers were used for analysis. Both lowest energy diastereomeric transition states contain an intramolecular hydrogen bond where the hydroxy substituent interacts with the iminyl nitrogen atom through a pseudoaxial positioning of the hydroxyl group in the developing five-membered ring. The transition state with the alkene acceptor in a pseudoequatorial position *cis* to the hydroxy group is lower in energy than the alternative structure possessing a pseudoaxial alkene. Based on the M06-2X relative enthalpy difference ($\Delta H_{120°C}$) between *cis* and *trans* transition states of 0.9 kcal/mol, the calculated 3:1 dr favoring the *cis* product is consistent with the observed 4.2:1 dr. UCCSD(T)/Def2-TZVP//UM06-2X/6-311++G** energies gave a similar enthalpy difference of 0.9 kcal/mol. Transition-state structures without an intramolecular hydrogen bond were found to be slightly higher in energy. For example, transition states with the hydroxyl group in a pseudoequatorial position were found to be 0.3 kcal/mol higher in energy. Also, the transition states similar to those shown in Figure 3a but with the O–H rotated away from the nitrogen and unable to hydrogen bond are about 0.6 kcal/mol higher in energy. Interestingly, structural analysis of the transition states in Figure 3a indicate that the hydrogen bond interaction itself does not account for the preference of *cis* over *trans*. The *trans* transition state has a slightly shorter, and expectedly stronger N–HO hydrogen bond distance. Therefore, to examine the differentiating effect in these transition states we replaced the entire vinyl with a hydrogen atom. Recalculation of the transition states showed nearly identical energies. Overall, this indicates that the *cis* configuration allows an unexpected and weak stabilizing interaction between a vinyl C–H and the hydroxyl group oxygen.

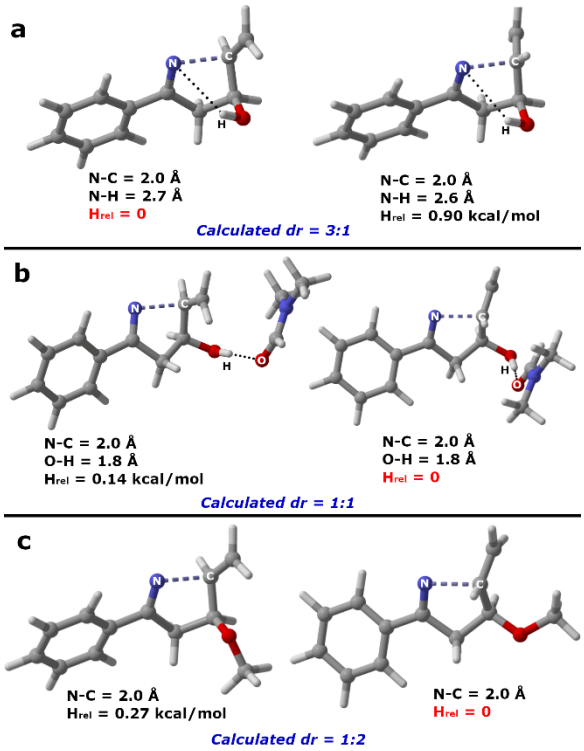

Figure 3. Computed transition structures for cyclizations of (a) **6i** with $PhCF_3$ as solvent, (b) **6i** with DMF as solvent, and (c) **8**.

To examine the impact of polar solvent on possible disruption of the intramolecular hydrogen bond, we included a single explicit DMF molecule in transition states derived from **6i** where the oxygen of DMF directly engages the hydroxyl group. We completed transition state searching by examining pseudoequatorial and pseudoaxial orientations of the hydroxyl group and the alkene acceptor and probing many orientations of DMF. Figure 3b displays the lowest-energy transition-state structures that were located. Consistent with the possibility of intramolecular hydrogen bonding being important for selectivity, these transition states both contain a pseudoequatorial hydroxy group. The M06-2X enthalpy difference between these DMF transition states is only 0.1 kcal/mol, which is consistent with the low observed dr (1.2:1) for the cyclization of **6i** performed in DMF.

Figure 3c shows the computed transition states for cyclization of β-methoxy-containing substrate **8**, which cannot form an intramolecular hydrogen bond. The transition state with a pseudoequatorial alkene, which affords the *trans*-disubstituted pyrroline **9**, was calculated to be slightly lower in enthalpy than the transition state with a pseudoaxial alkene. While this enthalpy difference is consistent with the observed

2.1:1 dr in favor of *trans*-**9**, the small magnitude of the difference suggests that this correlation with experiment should not be overinterpreted.

Cyclizations of α-hydroxy-substituted *O*-phenyloxime **6g** in polar solvents afforded **7g** with lower diastereoselectivity than was obtained using $PhCF_3$ (Table 3). All of the reactions were low-yielding, with the exact yields depending somewhat on the identity of the solvent. Microwave irradiation of α-methoxy-substituted substrate **10** furnished pyrroline **11** with negligible selectivity for the *trans* isomer (Scheme 5). While these results provide some evidence of intramolecular hydrogen bonding, the modest diastereoselectivity observed with $PhCF_3$ suggests that it is playing less of a role in cyclizations of **6g** than in cyclizations of β-hydroxy *O*-phenyloxime **6i**. It is possible that minimization of repulsion between the adjacent C=N and C–O dipoles of **6g**[34] could reduce the propensity of this substrate to form an intramolecular hydrogen bond.

Table 3. Cyclizations of 6g in Various Solvents

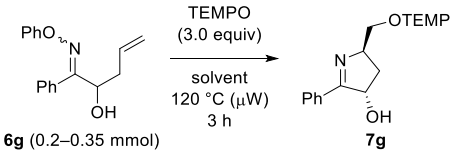

entry	solvent	yield (%)[a]	dr[b]
1	$PhCF_3$	34	2.6:1
2	DMF	11	1.3:1
3	CH_3OH	35	1.6:1
4	CH_3CN	21	1.8:1

[a]Isolated yield of major diastereomer. [b]Calculated from ^1H NMR spectra of reaction mixtures.

Scheme 5. Cyclization of α-OMe-Substituted *O*-Phenyloxime

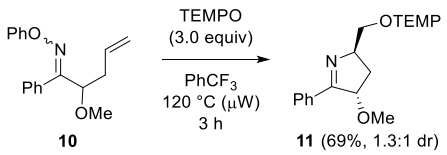

The successful correlation of calculated transition states of **6i** and **8** with their experimental dr values prompted us to examine the cyclization of **6g** in analogous fashion. Surprisingly, the calculated transition states for C–N bond formation of **6g** showed an 0.9 kcal/mol difference in energy favoring the minor *cis* isomer. Since the M06-2X calculated selectivity was qualitatively opposite to experiment, we calculated the UCCSD(T)/Def2-TZVP transition-state energies. The UCCSD(T) energies also showed a lower-energy transition state leading to the minor *cis* isomer. This prompted us to calculate NMR shielding tensors using the GIAO method to confirm stereoisomer assignment. These tensor calculations confirmed the assignment that the *trans* stereoisomer is generated in preference to the *cis* stereoisomer.

The inability of both DFT and CCSD(T) calculations to reproduce the observed stereochemical preference for cyclization of **6g** prompted us to consider that the formation of the C–N bond might be reversible and that the energy difference of the resulting cyclized radical intermediates or the final products controls the stereoisomer ratio. For the iminyl radical formed from **6g**, the C–N bond-forming step has an activation enthalpy ($\Delta H^{\ddagger}_{120°C}$) of 7.3 kcal/mol and is exothermic by 21.6 kcal/mol. The reverse barrier to regenerate the iminyl radical is 28.9 kcal/mol. While this is a relatively large reverse barrier, the estimated reverse rate constant from approximate transition state theory at 120 °C is 10^2/sec. Thus, reversibility of the iminyl radical cyclization step is feasible at elevated temperatures.

Figure 4 reports the Boltzmann-weighted relative enthalpies (the lowest 20 conformers) for the *cis* and *trans* isomers of the pyrroline adducts **7i**, **9**, **7g**, and **11**. For **7g**, which results from cyclization of **6g**, there is a thermodynamic enthalpy preference of 0.5 kcal/mol for the *trans* stereoisomer. While this energy difference might be overestimated by M06-2X, it does suggest the concept of partial thermodynamic control as a possible alternative to kinetic control by C–N bond-forming transition states. Consistent with the general idea of partial thermodynamic control, the relative enthalpies of stereoisomeric pyrroline products **7i**, **9**, **7g**, and **11** each show a preference for the experimentally identified major isomer (see Figure 4).

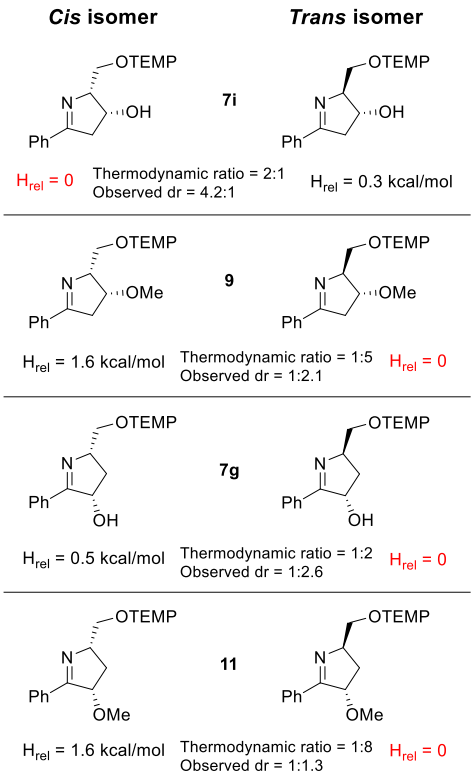

Figure 4. Relative enthalpies of major and minor diastereomers for **7i**, **9**, **7g**, and **11**.

The ability to perform microwave-promoted iminyl radical cyclizations at lower temperatures should expand the scope of the process, as some sensitive substrates might degrade at 120 °C. We reasoned that a radical precursor possessing an electron-donating group on the aryl ring of the oxime would exhibit a lower N–O bond dissociation energy (BDE) than our first-generation *O*-phenyloxime substrates due to increased stabilization of the aryloxy radical formed by homolysis. Accordingly, such substrates should undergo iminyl radical formation and cyclization at temperatures below 120 °C. To test this hypothesis, we synthesized *O*-arylhydroxylamine hydrochloride salt **12** bearing a *tert*-butyl group at the *para* position (Figure 5). This compound was readily accessible using Sharpless and Kelly's method[35] that we routinely employ to prepare *O*-phenylhydroxylamine hydrochloride. Compound **12** was amenable to condensation with ketones, and the resulting *O*-aryloximes were evaluated as substrates for iminyl radical cyclizations performed at lower temperatures.

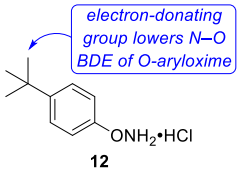

12

Figure 5. Second-generation *O*-arylhydroxylamine.

Microwave-promoted cyclizations of *O*-(*p-tert*-butyl)phenyloxime **13** were conducted in the presence of several different radical traps, and the results are summarized in Scheme 6. Initial studies with TEMPO trapping revealed that pyrroline **3b** was obtained in good yield (74%) when the reaction was performed at 100 °C. However, further reduction of the temperature to 85 °C resulted in a lower yield (53%). Accordingly, most of the cyclizations of **13** with other radical traps were carried out at 100 °C. The use of 2-iodopropane (**2e**) resulted in high yields of pyrroline **3e** (81%), although a slightly higher temperature (110 °C) was required. Xanthate **2g** was also a useful radical trap, delivering pyrroline **3g** in 50% yield. In contrast, allylsulfone **2a** and CCl_4 (**2c**) performed poorly, furnishing low yields of pyrrolines **3a** and **3c** even at the original reaction temperature of 120 °C. Only trace amounts of pyrroline **3f** could be detected in reactions employing sulfonyl azide **2f**, and none of the desired product was isolated. Benziodoxolone **2h** was also an ineffective trap for cyclizations of **13**, affording very low yields of pyrroline **3f**.

Scheme 6. Cyclizations of Second-Generation *O*-Aryloxime 13 with Various Radical Traps

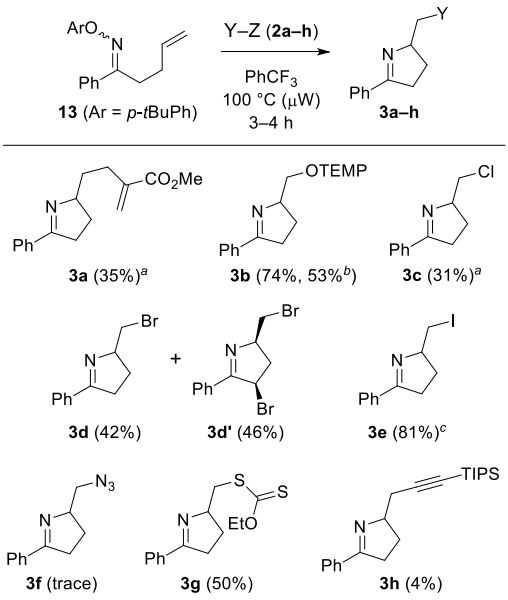

[a]120 °C, 2 h. [b]85 °C, 4 h. [c]110 °C, 4 h.

Microwave-promoted cyclizations of *O*-phenyloxime substrates were characterized by the presence of dark insoluble material, whereas the reaction mixtures derived from cyclizations of **13** were cleaner and

clearer in appearance. We suspect that the dark material could be derived from polymerization of the phenoxy radical that is formed in the initial N–O homolysis step. The bulkier *p-tert*-butylphenoxy radical generated in the homolysis of **13** would be expected to polymerize more slowly, thereby resulting in a cleaner reaction mixture. However, this would lead to higher concentrations of aryloxy radicals in solution that could either inhibit the desired reaction or degrade the products. The outcomes would likely depend on the relative rates of trapping the exocyclic radical intermediate as well as the relative stabilities of the pyrroline adducts.

Cyclizations of **13** conducted in the presence of CBr_4 (**2d**) provided further evidence for participation of the endogenous *p-tert*-butylphenoxy radical. Dibromide **3d'** was produced in 45% yield along with monobromide **3d** (42%). In contrast, analogous cyclizations of *O*-phenyloxime **1** with **2d** delivered **3d** in 73% yield and **3d'** in ca. 10% yield (see Figure 1, entry 4). The dibromide is presumably generated by abstraction of an α-hydrogen atom from **3d** followed by trapping of the resulting radical by CBr_4. Although this abstraction could be mediated by the $^{\bullet}CBr_3$ that is present in the reaction mixture, the different outcomes of cyclizations of **1** and **13** implicate the aryloxy radical. Nonetheless, further studies are needed to precisely define the role of the *p-tert*-butylphenoxy radical in the iminyl radical cyclizations of substrate **13**. Based on our results, it appears that the *p-tert*-butylphenyl-containing iminyl radical precursor affords better results (i.e., high-yielding reactions at lower temperatures) than the original phenyl-containing radical precursor with some radical traps but poorer results with others. Thus, selection of the appropriate cyclization substrate should be made on a case-by-case basis.

We next attempted to construct an *O*-(*p*-methoxy)phenyloxime in order to study the impact of a small and potent electron-donating group on microwave-promoted iminyl radical cyclizations. Whereas other *O*-aryloximes could be generated by pyridine-promoted condensation of a ketone and an *O*-(aryl)hydroxylamine,[16] in this case we were unable to prepare the requisite *O*-(*p*-methoxyphenyl)hydroxylamine. Solutions that presumably contained this compound rapidly turned dark upon concentration, suggesting that it is quite unstable. Thus, we employed an alternative route to the desired substrate as outlined in Scheme 7. Oxime **14** underwent Cu-promoted *O*-arylation[36] with *p*-

methoxyphenylboronic acid, delivering O-aryloxime **15** in modest yield. As anticipated, microwave-promoted N–O homolysis of **15** proceeded at a relatively low temperature (85 °C). However, a complex mixture ensued and pyrroline **3b** was obtained in poor yield. We were unable to characterize any byproducts or make any observations that would provide us with insights as to the reasons for this result, and the low-yielding synthesis of substrate **15** dampened our enthusiasm for further investigation.

Scheme 7. Synthesis and Cyclization of *O*-(*p*-Methoxy)phenyloxime 15

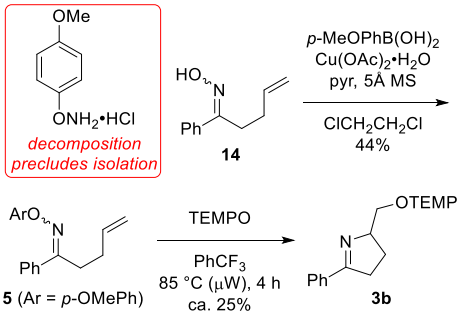

Our initial efforts to scale up the iminyl radical cyclizations involved *O*-phenyloxime **1**. Microwave irradiation of ca. 1 mmol of this compound in the presence of TEMPO furnished pyrroline **3b** in good yield (Scheme 8, eq 1). Interestingly, cyclization of **1** using conventional heating in an oil bath afforded a comparable yield (Scheme 8, eq 2). In contrast, Walton and co-workers obtained poor yields from conventionally heated reactions.[16] The successful execution of the cyclization of **1** in an oil bath prompted us to examine the cyclization of *O*-(*p*-*tert*-butyl)phenyloxime **13** with conventional heating, as this compound should presumably react at lower temperatures than **1**. Indeed, conducting the cyclization of **13** at 100 °C in an oil bath delivered pyrroline **3b** in virtually identical yield to the analogous reaction performed in the microwave reactor (Table 4, entry 1; cf. Scheme 6). Lowering the temperature to 90 °C resulted in a minor drop in yield (entry 2), while a more significant reduction in yield was observed at 85 °C (entry 3). Although the conventionally heated reactions are slower than the microwave-promoted reactions (presumably due to the efficient and uniform heating afforded by microwave irradiation), the ability to conduct iminyl radical cyclizations in an oil bath facilitates scale-up and renders the process accessible to researchers who do not possess a microwave reactor.

Scheme 8. Cyclizations on a Larger Scale and with Conventional Heating

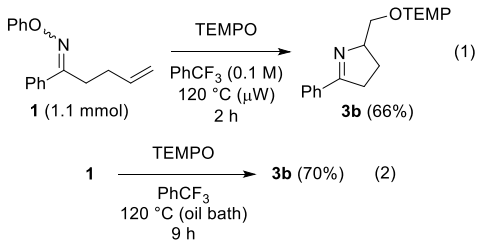

Table 4. Cyclizations of 13 with Conventional Heating

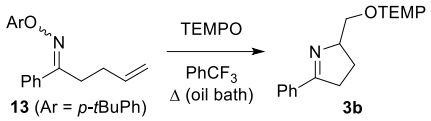

entry	temperature (°C)	time (h)	yield (%)
1	100	12	73
2	90	16	67
3	85	16	44

The success of the conventionally heated iminyl radical cyclizations prompted us to explore combining the *O*-aryloxime substrate synthesis and the cyclization steps into a one-pot process. After some investigation, we found that heating a solution of ketone **16** and *O*-arylhydroxylamine hydrochloride **12** in $PhCF_3$ at 40 °C induced the formation of *O*-aryloxime **13** (Scheme 9). Adding TEMPO to the solution and raising the temperature to 105 °C triggered iminyl radical formation, cyclization, and trapping, furnishing pyrroline **3b** in 42% yield. Although the yield is slightly lower than that of the corresponding two-step sequence involving isolation of **13**, this one-pot protocol should prove useful in cases where purification of the *O*-aryloxime substrate is either problematic or impractical.

Scheme 9. One-pot Oxime Ether Formation–Cyclization

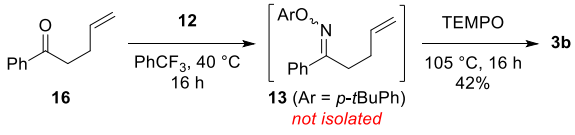

The microwave-promoted iminyl radical cyclizations produce functionalized pyrrolines, which are useful compounds that can be transformed in various ways as shown in Scheme 10. For example, Pd-catalyzed hydrogenation of **3b** furnished *cis*-pyrrolidine **17** selectively and in high yield (Scheme 10A). Reductions of **3b** using $NaBH(OAc)_3$ or $NaBH_3CN$ afforded **17** with lower yields and dr values. Tosylation of **17** and subsequent N–O bond cleavage[37] delivered primary alcohol **18**. Additionally, a Grignard reagent underwent diastereoselective addition to the less-hindered face of **3b**, generating pyrrolidine **19**. The terminal alkene of pyrroline **5** could also be manipulated, as exposure of this compound to methyl acrylate and the Grubbs second-generation ruthenium catalyst furnished enoate **20** (Scheme 10B). Two loadings were required to obtain high yields, as the basic imine is capable of coordinating and possibly decomposing the catalyst. Finally, osmium-catalyzed dihydroxylation[38] of **5** afforded diol **21** as a mixture of diastereomers (Scheme 10C). The ability to convert the pyrroline adducts of iminyl radical cyclizations into a range of products suggests a multitude of future applications.

Scheme 10. Transformations of Pyrroline Adducts

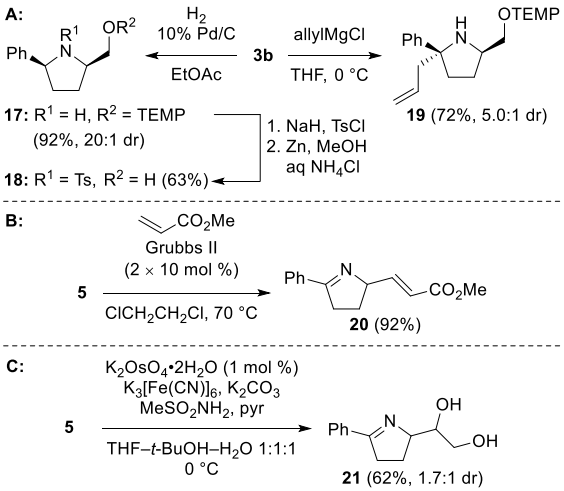

CONCLUSION

We have developed an efficient and operationally simple method for constructing pyrrolines via 5-*exo* iminyl radical cyclizations. The requisite radicals are generated by direct homolysis of the weak N–O bond of *O*-aryloximes, a process that can be promoted by either microwave irradiation or conventional heating. Catalysts and SET cycles are not required, enabling use of a diverse collection of radical traps

and giving the reaction a broad scope. *O*-aryloximes that are tethered to an allylic sulfide undergo a tandem cyclization–thiyl radical β-elimination that furnishes terminal alkenes. Cyclizations of substrates bearing hydroxy groups are moderately stereoselective, and experiments suggest that intramolecular hydrogen bonding may be playing a role. Computational studies provided support for intramolecular hydrogen bonding in some cases and suggested partial thermodynamic control of stereochemistry due to the potentially reversible cyclizations at elevated temperatures. *tert*-Butyl-substituted *O*-aryloximes were found to undergo N–O homolysis and subsequent cyclization at lower temperatures than the original *O*-phenyloxime substrates. This phenomenon is presumably due to the lower N–O BDE caused by the stabilizing effect of the *tert*-butyl group on the resulting aryloxy radical. These second-generation iminyl radical precursors can be used in a one-pot oxime ether formation–cyclization that is promoted by conventional heating. Finally, the pyrrolines that are produced by the cyclizations can be transformed in a variety of useful ways. We believe that these microwave- and thermally-promoted reactions will be widely employed by the organic synthesis community.

EXPERIMENTAL SECTION

General Details. Pyridine and THF were dried by passage through a solvent drying system employing activated alumina cylinders. Flash chromatography was carried out using 230 mesh silica gel. ^{1}H NMR spectra were obtained on Varian or Bruker 500 MHz spectrometers, with chloroform (7.27 ppm) or benzene (7.15 ppm) as internal references. Signals are reported as follows: s (singlet), d (doublet), t (triplet), q (quartet), quin (quintet), dd (doublet of doublets), ddd (doublet of doublet of doublets), m (multiplet). Coupling constants are reported in hertz (Hz). ^{13}C NMR spectra were obtained on Varian or Bruker spectrometers operating at 125 MHz, with chloroform (77.23 ppm) or benzene (127.7 ppm) as internal references. Infrared spectra were obtained on an FT-IR spectrometer. Mass spectral data were obtained using ESI mass spectrometry. Microwave-promoted reactions were carried out by irradiating sealed reaction mixtures inside a CEM Discover SP microwave reactor that was set at 200 W. Reactions employing conventional heating were performed in an oil bath. The preparation of compounds **1**, **4**, **5**, **6a**–**i**, **7a**–**i**, **17**, **18**, **19**, and **20** was described in our previous report.[19]

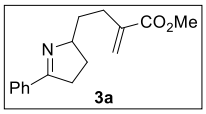

Methyl 2-methylene-4-(5-phenyl-3,4-dihydro-2*H*-pyrrol-2-yl)butanoate (3a). An oven-dried reaction vessel was charged with *O*-(*p*-*tert*-butyl)phenyl oxime **13** (17.3 mg, 0.0562 mmol), methyl 2-((phenylsulfonyl)methyl)acrylate (**2a**,[39] 85.8 mg, 0.357 mmol, 6.3 equiv), and $PhCF_3$ (2.0 mL), and was then sealed. The mixture was subjected to microwave irradiation (200 W) at 120 °C for 2 h, then cooled to rt and concentrated *in vacuo*. Flash chromatography (SiO_2, 0.9 × 13.8 cm, 2–25% EtOAc in hexanes gradient elution) afforded **3a** (5.0 mg, 0.0194 mmol, 35%) as a yellow oil. Spectral data were identical to the previously reported data.[19]

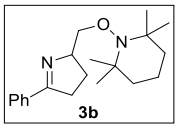

2,2,6,6-Tetramethyl-1-((5-phenyl-3,4-dihydro-2*H*-pyrrol-2-yl)methoxy) piperidine (3b). An oven-dried reaction vessel was charged with *O*-(*p*-*tert*-butyl)phenyl oxime **13** (30.3 mg, 0.0986 mmol), TEMPO (133.5 mg, 0.854 mmol, 8.7 equiv), and $PhCF_3$ (2 mL), and was then sealed. The mixture was subjected to microwave irradiation (200 W) at 100 °C for 4 h, then cooled to rt and concentrated *in vacuo*. Flash chromatography (SiO_2, 1 × 10 cm, 3–50% EtOAc in hexanes gradient elution) afforded **3b** (23.0 mg, 0.0731 mmol, 74%) as a brown–orange oil. Spectral data were identical to the previously reported data.[19]

Synthesis of 3b from 13 with conventional heating. A round-bottom flask was charged with **13** (33.7 mg, 0.110 mmol), TEMPO (163 mg, 1.04 mmol, 9.5 equiv), and $PhCF_3$ (2 mL). The resulting mixture was stirred at 100 °C under Ar for 12 h, then cooled to rt and concentrated *in vacuo.* Flash chromatography (SiO_2, 1.8 × 22 cm, 5–50% EtOAc in hexanes gradient elution) afforded **3b** (25.2 mg, 0.0801 mmol, 73%).

One-pot synthesis of 3b from ketone 16. A round-bottom flask was charged with 1-phenylpent-4-en-1-one[9] (**16**, 31.5 mg, 0.197 mmol), *p*-*tert*-$BuPhONH_2$•HCl (**12**, 58.5 mg, 0.290 mmol, 1.5 equiv), and $PhCF_3$ (5.9 mL). The resulting mixture was stirred at 40 °C under Ar for 16 h, then treated with

TEMPO (91.6 mg, 0.586 mmol, 3 equiv) and stirred at 105 °C for 16 h. It was then cooled to rt and concentrated *in vacuo.* Flash chromatography (SiO_2, 1.8 × 22 cm, 5–50% EtOAc in hexanes gradient elution) afforded **3b** (26.2 mg, 0.0833 mmol, 42%).

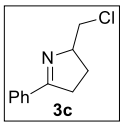

2-(Chloromethyl)-5-phenyl-3,4-dihydro-2*H*-pyrrole (3c). An oven-dried reaction vessel was charged with *O*-(*p-tert*-butyl)phenyl oxime **13** (16.4 mg, 0.0533 mmol), CCl_4 (30 μL, 47.7 mg, 0.310 mmol, 5.8 equiv), and $PhCF_3$ (1 mL), and was then sealed. The mixture was subjected to microwave irradiation (200 W) at 120 °C for 2 h, then cooled to rt and concentrated *in vacuo*. Flash chromatography (SiO_2, 0.9 × 13.5 cm, 2–20% EtOAc in hexanes gradient elution) afforded **3c** (3.2 mg, 0.0165 mmol, 31%) as a yellow–orange oil. Spectral data were identical to the previously reported data.[19]

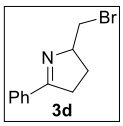

2-(Bromomethyl)-5-phenyl-3,4-dihydro-2*H*-pyrrole (3d). An oven-dried reaction vessel was charged with *O*-(*p-tert*-butyl)phenyl oxime **13** (30.4 mg, 0.0989 mmol), CBr_4 (346 mg, 1.04 mmol, 10.6 equiv), and $PhCF_3$ (2 mL), and was then sealed. The mixture was subjected to microwave irradiation (200 W) at 100 °C for 4 h, then cooled to rt and concentrated *in vacuo*. Flash chromatography (SiO_2, 1 × 10 cm, 3–30% EtOAc in hexanes gradient elution) afforded **3d** (10.0 mg, 0.0420 mmol, 42%) as a yellow oil. Spectral data were identical to the previously reported data.[19]

(2*R,4*R**)-4-Bromo-2-(bromomethyl)-5-phenyl-3,4-dihydro-2*H*-pyrrole** (**3d'**) was obtained as a byproduct (14.3 mg, 0.0451 mmol, 46% yield): ^{1}H NMR ($CDCl_3$, 500 MHz) δ 7.94 (d, *J* = 7.0 Hz, 2H), 7.51–7.43 (m, 3H), 5.31 (d, *J* = 7.0 Hz, 1H) 4.67–4.62 (m, 1H), 3.87 (dd, *J* = 10.5, 4.0 Hz, 1H), 3.79 (dd, *J* = 10.0, 6.5 Hz, 1H), 2.69 (dd, *J* = 14.5, 5.5 Hz, 1H), 2.38 (quin, *J* = 7.5 Hz, 1H); ^{13}C NMR ($CDCl_3$, 125 MHz) δ 172.0, 131.4, 128.7 (2C), 128.6, 128.4 (2C), 70.8, 48.1, 41.0, 36.0; IR (film) ν_{max} 2955, 2923, 2852, 1604, 1447 cm^{-1}; HRMS (ESI) *m/z*: $[M + H]^+$ Calcd for $C_{11}H_{11}NBr_2H$ 317.9311; Found 317.9310.

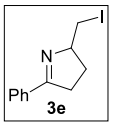

2-(Iodomethyl)-5-phenyl-3,4-dihydro-2*H*-pyrrole (3e). A reaction vessel was charged with *O*-(*p*-*tert*-butyl)phenyl oxime **13** (17.3 mg, 0.0563 mmol), 2-iodopropane (37 μL, 63 mg, 0.37 mmol, 6.6 equiv), and $PhCF_3$ (2 mL), and was then sealed. The mixture was subjected to microwave irradiation (200 W) at 110 °C for 4 h, then cooled to rt and concentrated *in vacuo*. Flash chromatography (SiO_2, 0.9 × 13.5 cm, 2–30% EtOAc in hexanes gradient elution) afforded **3e** (13.0 mg, 0.0456 mmol, 81%) as a yellow–orange oil. Spectral data were identical to the previously reported data.[19]

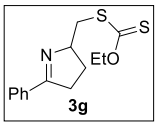

***O*-Ethyl *S*-((5-Phenyl-3,4-dihydro-2*H*-pyrrol-2-yl)methyl) carbonodithioate (3g).** An oven-dried reaction vessel was charged with *O*-(*p*-*tert*-butyl)phenyl oxime **13** (30.0 mg, 0.0976 mmol), xanthate **2g** (117 mg, 0.562 mmol, 5.8 equiv), and $PhCF_3$ (2 mL), and was then sealed. The mixture was subjected to microwave irradiation (200 W) at 100 °C for 4 h, then cooled to rt and concentrated *in vacuo*. Flash chromatography (SiO_2, 2 × 15 cm, 10–25% EtOAc in hexanes gradient elution) afforded **3g** (13.6 mg, 0.0487 mmol, 50%) as a yellow oil. Spectral data were identical to the previously reported data.[19]

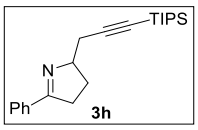

5-Phenyl-2-(3-(triisopropylsilyl)prop-2-yn-1-yl)-3,4-dihydro-2*H*-pyrrole (3h). An oven-dried reaction vessel was charged with *O*-(*p*-*tert*-butyl)phenyl oxime **13** (30.0 mg, 0.0976 mmol), 1-[(triisopropylsilyl)ethynyl]-1,2-benziodoxol-3(1*H*)-one[40] (**2h**, 79.7 mg, 0.186 mmol, 1.9 equiv), and $PhCF_3$ (2 mL), and was then sealed. The mixture was subjected to microwave irradiation (200 W) at 100 °C for 3 h, then cooled to rt and concentrated *in vacuo*. Flash chromatography (SiO_2, 2 × 15 cm, 1–50% EtOAc in hexanes gradient elution) afforded **3h** (1.2 mg, 0.0035 mmol, 4%) as a yellow oil. Spectral data were identical to the previously reported data.[19]

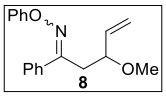

3-Methoxy-1-phenylpent-4-en-1-one *O*-phenyl oxime (8). A solution of *O*-phenyl oxime **6i**[19] (50.0 mg, 0.187 mmol) in anhydrous THF (5 mL) at rt under Ar was treated with NaH (60% dispersion in mineral oil, 9.0 mg, 0.23 mmol, 1.2 equiv) followed by CH_3I (25.0 μL, 57.0 mg, 0.402 mmol, 2.1 equiv). The mixture was then stirred at 40 °C under Ar for 20 h. The resulting yellow suspension was concentrated *in vacuo*, and the residue was treated with H_2O (1 mL) to quench the excess NaH. The mixture was extracted with $CHCl_3$ (2 × 15 mL), and the combined organic layers were dried (Na_2SO_4) and concentrated *in vacuo*. Flash chromatography (SiO_2, 2 × 14.5 cm, 2–5% EtOAc in hexanes gradient elution) afforded **8** (45.8 mg, 0.163 mmol, 87%) as a dark-brown viscous oil that was a 1.3:1 mixture of diastereomers: ^{1}H NMR ($CDCl_3$, 500 MHz, data for major diastereomer) δ 7.80–7.76 (m, 2H), 7.45–7.39 (m, 4H), 7.31–7.26 (m, 3H), 7.05–7.01 (m, 1H), 5.78–5.68 (m, 1H), 5.25–5.21 (m, 1H), 5.19–5.15 (m, 1H), 3.71 (q, *J* = 7.2 Hz, 1H), 3.20 (s, 3H), 3.01 (dd, *J* = 14.6, 7.8 Hz, 1H), 2.82 (dd, *J* = 14.6, 6.2 Hz, 1H); ^{13}C{^{1}H} NMR ($CDCl_3$, 125 MHz, data for major diastereomer) δ 159.3, 158.6, 137.4, 129.6, 129.3 (2C), 128.2 (2C), 127.9 (2C), 127.2, 122.0, 118.2, 114.7 (2C), 79.7, 56.3, 41.4; IR (film) ν_{max} 3054, 2926, 2853, 2360, 1594, 1492, 1445, 1375, 1265, 1215, 1102 cm^{-1}; HRMS (ESI) *m/z*: $[M + H]^+$ Calcd for $C_{18}H_{19}NO_2H$ 282.1489; Found 282.1493.

The following signals from the minor diastereomer were resolved in the ^{1}H NMR spectrum and were used to calculate the diastereomeric ratio: δ 4.05 (q, *J* = 7.2 Hz, 1H; corresponds to 3.71 ppm signal in major diastereomer), 3.24 (s, 3H; corresponds to 3.20 ppm signal in major diastereomer).

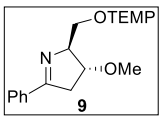

1-(((2*S,3*R**)-3-Methoxy-5-phenyl-3,4-dihydro-2*H*-pyrrol-2-yl)methoxy)-2,2,6,6-tetramethylpiperidine (9).** An oven-dried reaction vessel was charged with *O*-phenyl oxime **8** (21.9 mg, 0.0778 mmol), TEMPO (36.5 mg, 0.234 mmol, 3.0 equiv), and $PhCF_3$ (3 mL). The mixture was subjected to microwave irradiation (200 W) at 120 °C for 3 h, then cooled to rt and concentrated *in vacuo*. Flash chromatography (SiO_2, 2 × 14.5 cm, 20–30% EtOAc in hexanes gradient elution) afforded **9** (14.4 mg,

0.0418 mmol, 54%) as a brown viscous oil that was a 2.1:1 mixture of diastereomers. For the major diastereomer: ^{1}H NMR ($CDCl_3$, 500 MHz) δ 7.84 (dd, *J* = 7.9, 1.6 Hz, 2H), 7.44–7.38 (m, 3H), 4.45 (t, *J* = 4.2 Hz, 1H), 4.19 (d, *J* = 6.4 Hz, 1H), 4.13 (dd, *J* = 9.0, 3.6 Hz, 1H), 3.94 (dd, *J* = 9.0, 5.0 Hz, 1H), 3.39 (s, 3H), 3.19 (ddd, *J* = 17.7, 6.5, 1.1 Hz, 1H), 3.06 (dd, *J* = 17.6, 1.2 Hz, 1H), 1.48–1.34 (m, 4H), 1.32–1.26 (m, 2H), 1.21 (s, 3H), 1.10 (s, 3H), 1.07 (s, 3H), 0.87 (s, 3H); ^{13}C{^{1}H} NMR ($CDCl_3$, 125 MHz) δ 172.1, 134.4, 130.5, 128.4 (2C), 127.7 (2C), 81.7, 78.0, 77.2 (obscured by solvent), 59.9 (2C), 56.3, 42.2, 39.55, 39.50, 33.3, 32.9, 20.3, 20.1, 17.0; IR (film) ν_{max} 3331, 2925, 2851, 1606, 1515, 1456, 1374, 1359, 1262, 1132, 1073 cm^{-1}; HRMS (ESI) *m/z*: $[M + H]^+$ Calcd for $C_{21}H_{32}N_2O_2H$ 345.2537; Found 345.2542.

For the minor diastereomer: ^{1}H NMR ($CDCl_3$, 500 MHz): δ 7.84 (dd, *J* = 7.9, 1.6 Hz, 2H), 7.43–7.37 (m, 3H), 4.26–4.22 (m, 2H), 4.19–4.15 (m, 2H), 3.37 (s, 3H), 3.14 (dd, *J* = 16.6, 2.6 Hz, 1H), 2.99 (dd, *J* = 17.0, 5.8 Hz, 1H), 1.52–1.40 (m, 4H), 1.36–1.31 (m, 2H), 1.25 (s, 3H), 1.21 (s, 3H), 1.13 (s, 3H), 1.03 (s, 3H); ^{13}C{^{1}H} NMR ($CDCl_3$, 125 MHz) δ 172.0, 134.6, 130.5, 128.3 (2C), 127.6 (2C), 80.5, 74.4, 74.1, 59.8, 59.7, 57.5, 40.8, 39.7, 39.6, 32.9, 32.8, 20.1, 20.0, 17.1; IR (film) ν_{max} 3104, 3021, 2926, 2826, 1684, 1540, 1458, 1362, 1244, 1183 cm^{-1}; HRMS (ESI) *m/z*: $[M + H]^+$ Calcd for $C_{21}H_{32}N_2O_2H$ 345.2537; Found 345.2543.

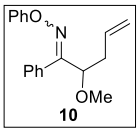

10

2-Methoxy-1-phenylpent-4-en-1-one *O*-phenyl oxime (10). A solution of *O*-phenyl oxime **6g**[19] (50.0 mg, 0.187 mmol) in anhydrous THF (10 mL) at rt under Ar was treated with NaH (60% dispersion in mineral oil, 9.0 mg, 0.23 mmol, 1.2 equiv) followed by CH_3I (25.0 μL, 57.0 mg, 0.402 mmol, 2.1 equiv). The mixture was then stirred at 40 °C under Ar for 20 h. The resulting yellow suspension was concentrated *in vacuo*, and the residue was treated with H_2O (1 mL) to quench the excess NaH. The mixture was extracted with $CHCl_3$ (2 × 15 mL), and the combined organic layers were dried (Na_2SO_4) and concentrated *in vacuo*. Flash chromatography (SiO_2, 2 × 14.5 cm, 2–5% EtOAc in hexanes gradient elution) afforded **10** (17.2 mg, 0.0611 mmol, 33%) as a dark-brown viscous oil that was a 1.2:1

mixture of diastereomers: ^{1}H NMR ($CDCl_3$, 500 MHz, data for major diastereomer) δ 7.86 (dd, *J* = 8.1, 1.6 Hz, 2H), 7.45–7.40 (m, 3H), 7.31–7.26 (m, 2H), 7.16 (dd, *J* = 8.7, 1.0 Hz, 2H), 7.01 (t, *J* = 7.3 Hz, 1H), 5.83–5.75 (m, 1H), 5.14–5.05 (m, 2H), 4.20 (t, *J* = 7.2 Hz, 1H), 3.52 (s, 3H), 2.44–2.37 (m, 1H), 2.31–2.24 (m, 1H); ^{13}C{^{1}H} NMR ($CDCl_3$, 125 MHz, data for major diastereomer) δ 161.5, 158.9, 133.4, 132.2, 129.6, 129.2 (2C), 128.3 (2C), 128.0 (2C), 122.4, 117.7, 114.9 (2C), 82.8, 56.9, 37.4; IR (film) ν_{max} 3059, 3027, 2928, 2821, 1593, 1489, 1455, 1318, 1215, 1100 cm^{-1}; HRMS (ESI) *m/z*: $[M + H]^+$ Calcd for $C_{18}H_{19}NO_2H$ 282.1489; Found 282.1491.

The following signals from the minor diastereomer were resolved in the ^{1}H NMR spectrum and were used to calculate the diastereomeric ratio: δ 7.05 (t, *J* = 7.2 Hz, 1H; corresponds to 7.01 ppm signal in major diastereomer), 5.93–5.84 (m, 1H; corresponds to 5.83–5.75 ppm signal in major diastereomer), 3.31 (s, 3H; corresponds to 3.52 ppm signal in major diastereomer), 2.72–2.65 (m, 1H; corresponds to 2.44–2.37 ppm signal in major diastereomer), 2.57–2.50 (m, 1H; corresponds to 2.31–2.24 ppm signal in major diastereomer).

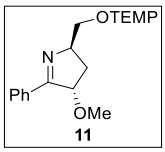

11

1-(((2*R,4*S**)-4-Methoxy-5-phenyl-3,4-dihydro-2*H*-pyrrol-2-yl)methoxy)-2,2,6,6-tetramethylpiperidine (11).** An oven-dried reaction vessel was charged with *O*-phenyl oxime **10** (17.2 mg, 0.0611mmol), TEMPO (28.6 mg, 0.183 mmol, 3.0 equiv), and $PhCF_3$ (2.5 mL). The mixture was subjected to microwave irradiation (200 W) at 120 °C for 3 h, then cooled to rt and concentrated *in vacuo*. Flash chromatography (SiO_2, 2 × 14.5 cm, 2–5% EtOAc in hexanes gradient elution) afforded **11** (14.5 mg, 0.0421 mmol, 69%) as a brown viscous oil that was a 1.3:1 mixture of diastereomers. For the major diastereomer: ^{1}H NMR ($CDCl_3$, 500 MHz) δ 7.94 (dd, *J* = 7.7, 1.9 Hz, 2H), 7.43–7.38 (m, 3H), 5.09–5.06 (m, 1H), 4.50–4.45 (m, 1H), 4.07 (dd, *J* = 8.8, 4.0 Hz, 1H), 3.97 (dd, *J* = 8.8, 4.7 Hz, 1H), 3.39 (s, 3H), 2.28 (ddd, *J* = 13.4, 7.7, 4.4 Hz, 1H), 2.17–2.11 (m, 1H), 1.48–1.37 (m, 4H), 1.33–1.26 (m, 2H), 1.20 (s, 3H), 1.10 (s, 6H), 0.91 (s, 3H); ^{13}C{^{1}H} NMR ($CDCl_3$, 125 MHz) δ 171.7, 133.4, 130.4, 128.3 (2C), 128.1

(2C), 85.9, 78.3, 70.0, 59.9 (2C), 56.1, 39.6 (2C), 33.2, 32.9, 32.5, 20.4, 20.0, 17.0; IR (film) ν_{max} 3056, 2925, 2853, 2356, 1729, 1617, 1558, 1448, 1374, 1360, 1263, 1131 cm^{-1}; HRMS (ESI) *m/z*: $[M + H]^+$ Calcd for $C_{21}H_{32}N_2O_2H$ 345.2537; Found 345.2541.

For the minor diastereomer: ^1H NMR ($CDCl_3$, 500 MHz) δ 7.92 (dd, *J* = 7.6, 2.0 Hz, 2H), 7.43–7.39 (m, 3H), 5.02 (dd, *J* = 7.2, 5.5 Hz, 1H), 4.30–4.24 (m, 1H), 4.13 (dd, *J* = 8.7, 4.6 Hz, 1H), 3.97 (dd, *J* = 8.8, 4.8 Hz, 1H), 3.39 (s, 3H), 2.46–2.39 (m, 1H), 2.05–2.00 (m, 1H), 1.48–1.37 (m, 4H), 1.32–1.25 (m, 2H), 1.25 (s, 3H), 1.20 (s, 3H), 1.10 (s, 6H), 0.91 (s, 3H); $^{13}C\{^1H\}$ NMR ($CDCl_3$, 125 MHz) δ 172.0, 133.3, 130.5, 128.4 (2C), 128.1 (2C), 85.4, 79.0, 69.1, 59.9 (2C), 56.1, 39.6 (2C), 33.2, 32.9, 32.5, 20.4, 20.0, 17.1; IR (film) ν_{max} 3058, 2921, 2853, 2356, 1734, 1619, 1558, 1448, 1374, 1358, 1263, 1131 cm^{-1}; HRMS (ESI) *m/z*: $[M + H]^+$ Calcd for $C_{21}H_{32}N_2O_2H$ 345.2537; Found 345.2539.

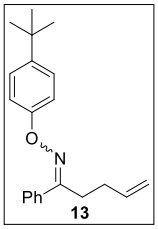

13

1-Phenylpent-4-en-1-one *O*-(4-(*tert*-butyl)phenyl) oxime (13). A solution of 1-phenylpent-4-en-1-one[9] (88.1 mg, 0.550 mmol) in anhydrous pyridine (2.0 mL) at rt under Ar was treated with *p-tert*-BuPhONH$_2$•HCl (**12**, 224 mg, 1.11 mmol, 2 equiv). The resulting mixture was stirred at 40 °C for 48 h, then diluted with H_2O (10 mL) and extracted with EtOAc (3 × 12 mL). The combined organic layers were washed with sat aq $CuSO_4$ (3 × 10 mL), dried (Na_2SO_4), and concentrated in vacuo. Flash chromatography (SiO_2, 2 × 15 cm, 2–50% EtOAc in hexanes gradient elution) afforded **13** (151 mg, 0.491 mmol, 89%) as a yellow-orange oil that was a 2.7:1 mixture of diastereomers. ^1H NMR ($CDCl_3$, 500 MHz, data for major diastereomer) δ 7.76–7.73 (m, 2H), 7.43–7.40 (m, 3H), 7.35 (d, *J* = 9.0 Hz, 2H), 7.20 (d, *J* = 9.0 Hz, 2H), 5.93–5.82 (m, 1H), 5.08 (dd, *J* = 17.0, 1.5 Hz, 1H), 5.00 (dd, *J* = 10.0, 1.5 Hz, 1H), 3.03 (t, *J* = 7.8 Hz, 2H), 2.40 (q, *J* = 7.3 Hz, 2H), 1.32 (s, 9H); $^{13}C\{^1H\}$ NMR ($CDCl_3$, 125 MHz, data for major diastereomer) δ 160.7, 157.3, 145.0, 137.3, 129.6, 128.5 (2C), 128.2, 126.7 (2C), 126.0 (2C), 115.3,

114.5 (2C), 34.2, 31.5 (3C), 30.7, 26.6; IR (film) ν_{max} 3062, 2958, 2961, 2867, 1604, 1506, 1225 cm^{-1}; HRMS (ESI) *m/z*: $[M + H]^+$ Calcd for $C_{21}H_{25}NOH$ 308.2009; Found 308.2016.

The following signals from the minor diastereomer were resolved in the ^1H NMR spectrum of **13** and were used to calculate the diastereomeric ratio: δ 7.30 (d, *J* = 8.8 Hz, 2H; corresponds to 7.35 ppm signal in major diastereomer), 7.07 (d, *J* = 8.8 Hz, 2H; corresponds to 7.20 ppm signal in major diastereomer), 2.77 (t, *J* = 7.6 Hz, 2H; corresponds to 3.03 ppm signal in major diastereomer), 2.32 (q, *J* = 7.2 Hz, 2H; corresponds to 2.40 ppm signal in major diastereomer).

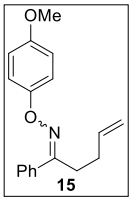

1-Phenylpent-4-en-1-one *O*-(4-methoxyphenyl) oxime (15). To a solution of oxime **14**[41] (75.0 mg, 0.428 mmol) in anhydrous dichloroethane (7.0 mL) was added 4-methoxyphenylboronic acid (130.0 mg, 0.856 mmol, 2 equiv), $Cu(OAc)_2•H_2O$ (85.6 mg, 0.429 mmol, 1 equiv), powdered 5 Å molecular sieves (116.8 mg), and pyridine (77 μL, 75.6 mg, 0.956 mmol, 2.2 equiv) while stirring. Upon addition of pyridine, the reaction mixture changed color from blue-green to brown. The resulting mixture was stirred at rt for 72 h in a loosely-capped vial, then filtered twice and concentrated *in vacuo.* Flash chromatography (SiO_2, 2 × 14.5 cm, 1–20% EtOAc in hexanes gradient elution) afforded **15** (53.0 mg, 0.188 mmol, 44%) as a pale-yellow oil that was a 3.8:1 mixture of diastereomers. ^1H NMR ($CDCl_3$, 500 MHz, data for major diastereomer) δ 7.97 (d, *J* = 7.3 Hz, 2H), 7.57 (t, *J* = 7.4 Hz, 1H), 7.47 (t, *J* = 7.6 Hz, 2H), 7.20 (d, *J* = 9.0 Hz, 2H), 6.88 (d, *J* = 9.0 Hz, 2H), 5.95–5.86 (m, 1H), 5.09 (dd, *J* = 17.2 Hz, 1.6 Hz, 1H), 5.02 (d, *J* = 10.2 Hz, 1H), 3.80 (s, 3H), 3.09 (t, *J* = 7.4 Hz, 2H), 2.51 (q, *J* = 7.1 Hz, 2H); $^{13}C\{^1H\}$ NMR ($CDCl_3$, 125 MHz, data for major diastereomer) δ 166.0, 160.5, 156.0, 137.3, 133.0, 128.6 (2C), 128.0 (2C), 126.4, 120.6, 117.1, 115.3 (2C), 114.8, 55.6, 37.7, 28.1; IR (film) ν_{max} 3064, 2958, 2957, 2925, 2854, 1688, 1500, 1229 cm^{-1}; HRMS (ESI) *m/z*: $[M + H]^+$ Calcd for $C_{18}H_{19}NO_2H$ 282.1489; Found 282.1481.

The following signals from the minor diastereomer were resolved in the ^{1}H NMR spectrum and were used to calculate the diastereomeric ratio: δ 7.74–7.71 (m, 2H; corresponds to 7.97 ppm signal in major diastereomer), 7.43–7.40 (m, 3H; corresponds to 7.57 and 7.47 ppm signals in major diastereomer), 3.03 (t, J = 7.9 Hz, 2H; corresponds to 3.09 ppm signal in major diastereomer), 2.40 (q, J = 7.7 Hz, 2H; corresponds to 2.51 ppm signal in major diastereomer).

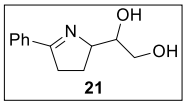

21

1-(5-Phenyl-3,4-dihydro-2*H*-pyrrol-2-yl)ethane-1,2-diol (21). A solution of $K_3[Fe(CN)_6]$ (132 mg, 0.401 mmol, 3.0 equiv), K_2CO_3 (55.4 mg, 0.401 mmol, 3 equiv), and pyridine (one drop, ca. 50 μL) in *t*BuOH–THF–H_2O (1:1:1, 1.5 mL) at 0 °C was treated with K_2OsO_4•$2H_2O$ (0.5 mg, 0.0014 mmol, 1.0 mol %) and methanesulfonamide (12.7 mg, 0.134 mmol, 1 equiv). The resulting mixture was stirred at 0 °C for 5 min, then treated with **5** (22.9 mg, 0.134 mmol) and stirred at 0 °C for 24 h. The reaction was quenched by the addition of solid Na_2SO_3 (120 mg). The mixture was filtered through Celite (washed with 40 mL EtOAc), washed with brine (2 × 10 mL), dried (Na_2SO_4) and concentrated *in vacuo*. Flash chromatography (SiO_2, 2 × 14.5 cm, 10–15% MeOH in CH_2Cl_2 gradient elution) afforded **21** (16.9 mg, 0.0823 mmol, 62%) as a white film that was a 1.7:1 mixture of diastereomers: ^{1}H NMR ($CDCl_3$, 500 MHz, data for major diastereomer) δ 7.82 (d, J = 7.6 Hz, 2H), 7.47–7.39 (m, 3H), 4.72 (br s, 1H), 4.25 (q, J = 5.8 Hz, 1H), 3.91 (q, J = 5.6 Hz, 1H), 3.86 (dd, J = 11.0, 5.0 Hz, 1H), 3.76 (dd, J = 11.0, 6.0 Hz, 1H), 3.09–3.05 (m, 1H), 2.96–2.88 (m, 1H), 2.24–2.18 (m, 1H), 1.97–1.89 (m, 1H), 1.62 (br s, 1H); ^{13}C{^{1}H} NMR ($CDCl_3$, 125 MHz, data for major diastereomer) δ 174.7, 133.8, 130.9, 128.5 (2C), 127.8 (2C), 76.5, 74.5, 65.4, 35.1, 24.8; IR (film) ν_{max} 3583, 3107, 2996, 2923, 2359, 2341, 1704, 1612, 1470, 1280, 1267, 1159 cm^{-1}; HRMS (ESI) *m/z*: $[M + H]^+$ Calcd for $C_{12}H_{15}NO_2H$ 206.1176; Found 206.1169.

The following signal from the minor diastereomer was resolved in the ^{1}H NMR spectrum and were used to calculate the diastereomeric ratio: δ 4.40–4.33 (m, 1H; corresponds to 4.25 ppm signal in major diastereomer).

Data Availability Statement. The data underlying this study are available in the published article and its online supporting information.

Supporting Information Available. Summary of diagnostic NOE correlations used to determine relative stereochemistry of **7d**, **7g**, **7h**, **7i**, **9**, **11**, **3d'**, **17**, and **19**; copies of ^{1}H and ^{13}C NMR spectra for all new compounds and known compounds prepared by new methods; a text file of all computed molecule Cartesian coordinates in a format for convenient visualization. This material is available free of charge via the Internet at http://pubs.acs.org.

Acknowledgment. We thank the National Science Foundation (CHE-1856530), the donors of the American Chemical Society Petroleum Research Fund (55514-ND1), and Brigham Young University (Undergraduate Research Awards to T.J.N., G.A.N., and D.D.J.) for financial support.

REFERENCES

(1) (a) Walton, J. C. Synthetic Strategies for 5- and 6-Membered Ring Azaheterocycles Facilitated by Iminyl Radicals. *Molecules* **2016**, *21*, 660. (b) Jackman, M. M.; Cai, Y.; Castle, S. L. Recent Advances in Iminyl Radical Cyclizations. *Synthesis* **2017**, *49*, 1785–1795. (c) Lei, J.; Li, D.; Zhu, Q. Synthesis of Nitrogen-Containing Heterocycles via Imidoyl or Iminyl Radical Intermediates. *Top. Heterocycl. Chem.* **2018**, *54*, 285–320. (d) Yin, W.; Wang, X. Recent Advances in Iminyl Radical-Mediated Catalytic Cyclizations and Ring-Opening Reactions. *New. J. Chem.* **2019**, *43*, 3254–3264. (e) Chen, C.; Zhao, J.; Shi, X.; Liu, L.; Zhu, Y.-P.; Sun, W.; Zhu, B. Recent Advances in Cyclization Reactions of Unsaturated Oxime Esters (Ethers): Synthesis of Versatile Functionalized Nitrogen-Containing Scaffolds. *Org. Chem. Front.* **2020**, *7*, 1948–1969. (f) Krylov, I. B.; Segida, O. O.; Budnikov, A. S.; Terent'ev, A. O. Oxime-Derived Iminyl Radicals in Selective Processes of Hydrogen Atom Transfer and Addition to Carbon–Carbon π-Bonds. *Adv. Synth. Catal.* **2021**, *363*, 2502–2528.

(2) (a) Zard, S. Z. Recent Progress in the Generation and Use of Nitrogen-Centred Radicals. *Chem. Soc. Rev.* **2008**, *37*, 1603–1618. (b) Xiong, T.; Zhang, Q. New Amination Strategies Based on Nitrogen-Centered Radical Chemistry. *Chem. Soc. Rev.* **2016**, *45*, 3069–3087. (c) McCombie, S. W.; Quiclet-Sire, B.; Zard, S. Z.; Blakemore, P. R. Cyclization Reactions of Nitrogen-Centered Radicals. *Org. React.* (Hoboken, NJ, U. S.) **2021**, *108*, DOI:10.1002/0471264180.or108.01. (d) Kwon, K.; Simons, R. T.; Nandakumar, M.; Roizen, J. L. Strategies to Generate Nitrogen-centered Radicals That May Rely on Photoredox Catalysis: Development in Reaction Methodology and Applications in Organic Synthesis. *Chem. Rev.* **2022**, *122*, 2353–2428.

(3) (a) Forrester, A. R.; Gill, M.; Sadd, J. S.; Thomson, R. H. New Chemistry of Iminyl Radicals. *J. Chem. Soc., Chem. Commun.* **1975**, 291–292. (b) Atmaram, S.; Forrester, A. R.; Gill, M.; Thomson, R. H. Iminyls. Part 9. Intramolecular Addition of an Iminyl to an Alkene. *J. Chem. Soc., Perkin Trans. 1* **1981**, 1721–1724.

(4) (a) Boivin, J.; Fouquet, E.; Zard, S. Z. Iminyl Radicals: Part I. Generation and Intramolecular Capture by an Olefin. *Tetrahedron* **1994**, *50*, 1745–1756. (c) Boivin, J.; Fouquet, E.; Schiano, A.-M.; Zard, S. Z. Iminyl Radicals: Part III. Further Synthetically Useful Sources of Iminyl Radicals. *Tetrahedron* **1994**, *50*, 1769–1776. (b) Boivin, J.; Callier-Dublanchet, A.-C.; Quiclet-Sire, B.; Schiano, A.-M.; Zard, S. Z. Iminyl, Amidyl, and Carbamyl Radicals from O-Benzoyl Oximes and O-Benzoyl Hydroxamic Acid Derivatives. *Tetrahedron* **1995**, *51*, 6517–6528. (c) Gagosz, F.; Zard, S. Z. Generation and Capture of Iminyl Radicals from Ketoxime Xanthates. *Synlett* **1999**, 1978–1980. (d) Bingham, M.; Moutrille, C.; Zard, S. Z. A Simple Route to Functionalized Δ^1-Pyrrolines. *Heterocycles* **2014**, *88*, 953–960.

(5) Lin, X.; Artman, G. D., III; Stien, D.; Weinreb, S. M. Development of Efficient New Methodology for Generation, Cyclization and Functional Trapping of Iminyl and Amidyl Radicals. *Tetrahedron* **2001**, *57*, 8779–8791.

(6) (a) Davies, J.; Booth, S. G.; Essafi, S.; Dryfe, R. A. W.; Leonori, D. Visible-Light-Mediated Generation of Nitrogen-Centered Radicals: Metal-Free Hydroimination and Iminohydroxylation Cyclization Reactions. *Angew. Chem., Int. Ed.* **2015**, *54*, 14017–14021. (b) Yang, H.-B.; Selander, N. Divergent Iron-Catalyzed Coupling of *O*-Acyloximes with Silyl Enol Ethers. *Chem. - Eur. J.* **2017**, *23*, 1779–1783. (c) Cai, S.-H.; Xie, J.-H.; Song, S.; Ye, L.; Feng, C.; Loh, T.-P. Visible-Light Promoted Carboimination of Unactivated Alkenes for the Synthesis of Densely Functionalized Pyrroline Derivatives. *ACS Catal.* **2016**, *6*, 5571–5574. (d) Guo, K.; Zhang, H.; Cao, S.; Gu, C.; Zhou, H.; Li, J.; Zhu, Y. Copper-Catalyzed Domino Cyclization/Trifluoromethylthiolation of Unactivated Alkenes: Access to SCF_3-Containing Pyrrolines. *Org. Lett.* **2018**, *20*, 2261–2264. (e) Shimbayashi, T.; Nakamoto, D.; Okamoto, K.; Ohe, K. Facile Construction of Tetrahydropyrrolizines by Iron-Catalyzed Double Cyclization of Alkene-Tethered Oxime Esters with 1,2-Disubstituted Alkenes. *Org. Lett.* **2018**, *20*, 3044–3048. (f) Chen, C.; Bao, Y.; Zhao, J.; Zhu, B. Silver-Promoted Cascade Radical Cyclization of γ,δ-Unsaturated Oxime Esters with P(O)H Compounds: Synthesis of Phosphorylated Pyrrolines. *Chem. Commun.* **2019**, *55*, 14697–14700. (g) Wang, L.; Wang, C. Copper-Catalyzed Diamination of Oxime Ester-Tethered Unactivated Alkenes with Unprotected Amines. *J. Org. Chem.* **2019**, *84*, 6547–6556. (h) Zhang, Y.; Yin, Z.; Wang, H.; Wu, X.-F. Iron-Catalyzed Carbonylative Cyclization of γ,δ-Unsaturated Aromatic Oxime Esters to Functionalized Pyrrolines. *Chem. Commun.* **2020**, *56*, 7045–7048. (i) Shen, X.; Huang, C.; Yuan, X.-A.; Yu, S. Diastereoselective and Stereodivergent Synthesis of 2-Cinnamylpyrrolines Enabled by Photoredox-Catalyzed Iminoalkenylation of Alkenes. *Angew. Chem., Int. Ed.* **2021**, *60*, 9672–9679.

(7) Alternatively, the catalyst can be turned over via reduction by the radical trap or an external reagent. This strategy also limits the types of trapping agents that can be used. For examples, see: (a) Wang, D.-X.; Cai, S.-H.; Liu, H.; Ye, L.; Zhu, C.; Feng, C. Visible-Light-Induced Iminothiolation of Unactivated Alkenes. *Asian J. Org. Chem.* **2021**, *10*, 1386–1389. (b) Chen, B.;

He, H.; Xu, J.; Guo, K.; Xu, N.; Chen, K.; Zhu, Y. Transition-Metal-Free Visible Light-Induced Imino-trifluoromethylation of Unsaturated Oxime Esters: A Facile Access to CF_3-Tethered Pyrrolines. *Asian J. Org. Chem.* **2021**, *10*, 2360–2364.

(8) Jiang, H.; Studer, A. Iminyl-Radicals by Oxidation of α-Imino-Oxy Acids: Photoredox-Neutral Alkene Carboimination for the Synthesis of Pyrrolines. *Angew. Chem., Int. Ed.* **2017**, *56*, 12273–12276.

(9) Davies, J.; Sheikh, N. S.; Leonori, D. Photoredox Imino Functionalizations of Olefins. *Angew. Chem., Int. Ed.* **2017**, *56*, 13361–13365.

(10) (a) Tu, J.-L.; Liu, J.-L.; Tang, W.; Su, M.; Liu, F. Radical Aza-Cyclization of α-Imino-oxy Acids for Synthesis of Alkene-Containing *N*-Heterocycles via Dual Cobaloxime and Photoredox Catalysis. *Org. Lett.* **2020**, *22*, 1222–1226. (b) Yan, X.; Li, X.; Wang, Y.; Dai, Y.; Yan, X.; Zhao, D.; Xu, X. Iminyl-Radical-Mediated C–C Cleavage/Amination and Alkene Iminoamination Enabled by Visible-Light-Induced Cerium Catalysis. *ACS Sustainable Chem. Eng.* **2021**, *9*, 101–105.

(11) For alternative methods of generating iminyl radicals, see: (a) Usami, K.; Yamaguchi, E.; Tada, N.; Itoh, A. Visible-Light-Mediated Iminyl Radical Generation from Benzyl Oxime Ether: Synthesis of Pyrroline via Hydroimination Cyclization. *Org. Lett.* **2018**, *20*, 5714–5717. (b) Zheng, D.; Jana, K.; Alasmary, F. A.; Daniluc, C. G.; Studer, A. Transition-Metal-Free Intramolecular Radical Aminoboration of Unactivated Alkenes. *Org. Lett.* **2021**, *23*, 7688–7692. (c) Zhang, M.; Zhang, Z.; He, Y.; Zou, T.; Qi, Z.; Fu, Q.; Wei, J.; Lu, J.; Wei, S.; Yi, D. Photocatalytic Deoxygenative Carboimination towards Functionalized Pyrrolines by Using Unstrained γ,δ-Unsaturated Oximes. *Adv. Synth. Catal.* **2021**, *363*, 2110–2116.

(12) (a) Schann, S.; Bruban, V.; Pompermayer, K.; Feldman, J.; Pfeiffer, B.; Renard, P.; Scalbert, E.; Bousquet, P.; Ehrhardt, J.-D. Synthesis and Biological Evaluation of Pyrrolinic Isosteres of

Rilmenidine. Discovery of *cis*-/*trans*-Dicyclopropylmethyl-(4,5-dimethyl-4,5-dihydro-3*H*-pyrrol-2-yl)-amine (LNP 509), an I_1 Imidazoline Receptor Selective Ligand with Hypotensive Activity. *J. Med. Chem.* **2001**, *44*, 1588–1593. (b) Adams, A.; De Kimpe, N. Chemistry of 2-Acetyl-1-pyrroline, 6-Acetyl-1,2,3,4-tetrahydropyridine, 2-Acetyl-2-thiazoline, and 5-Acetyl-2,3-dihydro-4*H*-thiazine: Extraordinary Maillard Flavor Compounds. *Chem. Rev.* **2006**, *106*, 2299–2319. (c) Pearson, M. S. M.; Floquet, N.; Bello, C.; Vogel, P.; Plantier-Royon, R.; Szymoniak, J.; Bertus, P.; Behr, J.-B. The Spirocyclopropyl Moiety as a Methyl Surrogate in the Structure of L-Fucosidase and L-Rhamnosidase Inhibitors. *Bioorg. Med. Chem.* **2009**, *17*, 8020–8026.

(13) Vitaku, E.; Smith, D. T.; Njardarson, J. T. Analysis of the Structural Diversity, Substitution Patterns, and Frequency of Nitrogen Heterocycles among U.S. FDA Approved Pharmaceuticals. *J. Med. Chem.* **2014**, *57*, 10257–10274.

(14) (a) Uchiyama, K.; Hayashi, Y.; Narasaka, K. Synthesis of Dihydropyrroles by the Intramolecular Addition of Alkylideneaminyl Radicals Generated from *O*-2,4-Dinitrophenyloximes of γ,δ-Unsaturated Ketones. *Tetrahedron* **1999**, *55*, 8915–8930. (b) Narasaka, K. Synthesis of Azaheterocycles from Oxime Derivatives. *Pure Appl. Chem.* **2003**, *75*, 19–28.

(15) Blake, J. A.; Pratt, D. A.; Lin, S.; Walton, J. C.; Mulder, P.; Ingold, K. U. Thermolyses of *O*-Phenyl Oxime Ethers. A New Source of Iminyl Radicals and a New Source of Aryloxyl Radicals. *J. Org. Chem.* **2004**, *69*, 3112–3120.

(16) (a) Portella-Cubillo, F.; Scott, J. S.; Walton, J. C. Microwave-Assisted Preparations of Dihydropyrroles from Alkenone *O*-Phenyl Oximes. *Chem. Commun.* **2007**, 4041–4043. (b) Portella-Cubillo, F.; Scott, J. S.; Walton, J. C. Microwave-Assisted Syntheses of *N*-Heterocycles Using Alkenone-, Alkynone- and Aryl-Carbonyl *O*-Phenyl Oximes: Formal Synthesis of Neocryptolepine. *J. Org. Chem.* **2008**, *73*, 5558–5565.

(17) Cai, Y.; Jalan, A.; Kubosumi, A. R.; Castle, S. L. Microwave-Promoted Tin-Free Iminyl Radical Cyclization with TEMPO Trapping: A Practical Synthesis of 2-Acylpyrroles. *Org. Lett.* **2015**, *17*, 488–491.

(18) Jackman, M. M.; Im, S.; Bohman, S. R.; Lo, C. C. L.; Garrity, A. L.; Castle, S. L. Synthesis of Functionalized Nitriles via Microwave-Promoted Fragmentations of Cyclic Iminyl Radicals. *Chem. - Eur. J.* **2018**, *24*, 594–598.

(19) Singh, J.; Nickel, G. A.; Cai, Y.; Jones, D. D.; Nelson, T. J.; Small, J. E.; Castle, S. L. Synthesis of Functionalized Pyrrolines via Microwave-Promoted Iminyl Radical Cyclizations. *Org. Lett.* **2021**, *23*, 3970–3974.

(20) Rouquet, G.; Robert, F.; Méreau, R.; Castet, F.; Landais, Y. Allylsilanes in "Tin-free" Oximation, Alkenylation, and Allylation of Alkyl Halides. *Chem. - Eur. J.* **2011**, *17*, 13904–13911.

(21) Yayla, H. G.; Wang, H.; Tarantino, K. T.; Orbe, H. S.; Knowles, R. R. Catalytic Ring-Opening of Cyclic Alcohols Enabled by PCET Activation of Strong O–H Bonds. *J. Am. Chem. Soc.* **2016**, *138*, 10794–10797

(22) Hou, T.; Lu, P.; Li, P. Visible-Light-Mediated Benzylic sp^3 C–H Bond Functionalization to C–Br or C–N Bond. *Tetrahedron Lett.* **2016**, *57*, 2273–2276.

(23) Bovino, M. T.; Chemler, S. R. Catalytic Enantioselective Alkene Aminohalogenation/Cyclization Involving Atom Transfer. *Angew. Chem., Int. Ed.* **2012**, *51*, 3923–3927.

(24) Panchaud, P.; Chabaud, L.; Landais, Y.; Ollivier, C.; Renaud, P.; Zigmantas, S. Radical Amination with Sulfonyl Azides: A Powerful Method for the Formation of C–N Bonds. *Chem. - Eur. J.* **2004**, *10*, 3606–3614.

(25) Quiclet-Sire, B.; Zard, S. Z. Fun with Radicals: Some New Perspectives for Organic Synthesis. *Pure Appl. Chem.* **2011**, *83*, 519–551.

(26) (a) Zhdankin, V. V.; Kuehl, C. J.; Krasutsky, A. P.; Bolz, J. T.; Simonsen, A. J. 1-(Organosulfonyloxy)-3(1*H*)-1,2-benziodoxoles: Preparation and Reactions with Alkynyltrimethylsilanes. *J. Org. Chem.* **1996**, *61*, 6547–6551. (b) Liu, X.; Yu, L.; Luo, M.; Zhu, J.; Wei, W. Radical-Induced Metal-Free Alkynylation of Aldehydes by Direct C–H Activation. *Chem. - Eur. J.* **2015**, *21*, 8745–8749.

(27) Rueda-Becerril, M.; Chatalova Sazepin, C.; Leung, J. C. T.; Okbinoglu, T.; Kennepohl, P.; Paquin, J.-F.; Sammis, G. M. Fluorine Transfer to Alkyl Radicals. *J. Am. Chem. Soc.* **2012**, *134*, 4026–4029.

(28) (a) Boger, D. L.; Wysocki, R. J., Jr.; Ishizaki, T. Synthesis of *N*-(Phenylsulfonyl)-CI, *N*-((*tert*)-Butyloxy)carbonyl)-CI, CI-CDPI$_1$, and CI-CDPI$_2$: CC-1065 Functional Analogues Incorporating the Parent 1,2,7,7a-Tetrahydrocycloprop[1,2-*c*]indol-4-one (CI) Left-Hand Subunit. *J. Am. Chem. Soc.* **1990**, *112*, 5230–5240. (b) Parker, K. A.; Fokas, D. Convergent Synthesis of (±)-Dihydroisocodeine in 11 Steps by the Tandem Radical Cyclization Strategy. A Formal Total Synthesis of (±)-Morphine. *J. Am. Chem. Soc.* **1992**, *114*, 9688–9689.

(29) In our preliminary publication (ref. 19), we incorrectly reported the dr of **7g** as 15:1 and **7i** as >20:1. These errors were due to our initial failure to correctly identify the minor diastereomers in the ^{1}H NMR spectra of the crude reaction mixtures.

(30) Frisch, M. J.; Trucks, G. W.; Schlegel, H. B.; Scuseria, G. E.; Robb, M. A.; Cheeseman, J. R.; Scalmani, G.; Barone, V.; Petersson, G. A.; Nakatsuji, H.; Li, X.; Caricato, M.; Marenich, A. V.; Bloino, J.; Janesko, B. G.; Gomperts, R.; Mennucci, B.; Hratchian, H. P.; Ortiz, J. V.; Izmaylov, A. F.; Sonnenberg, J. L.; Williams-Young, D.; Ding, F.; Lipparini, F.; Egidi, F.; Goings, J.; Peng, B.; Petrone, A.; Henderson, T.; Ranasinghe, D.; Zakrzewski, V. G.; Gao, J.; Rega, N.; Zheng, G.; Liang, W.; Hada, M.; Ehara, M.; Toyota, K.; Fukuda, R.; Hasegawa, J.; Ishida, M.; Nakajima, T.; Honda, Y.; Kitao, O.; Nakai, H.; Vreven, T.; Throssell, K.; Montgomery, J. A., Jr.; Peralta, J. E.;

Ogliaro, F.; Bearpark, M. J.; Heyd, J. J.; Brothers, E. N.; Kudin, K. N.; Staroverov, V. N.; Keith, T. A.; Kobayashi, R.; Normand, J.; Raghavachari, K.; Rendell, A. P.; Burant, J. C.; Iyengar, S. S.; Tomasi, J.; Cossi, M.; Millam, J. M.; Klene, M.; Adamo, C.; Cammi, R.; Ochterski, J. W.; Martin, R. L.; Morokuma, K.; Farkas, Ö.; Foresman, J. B.; Fox, D. J. *Gaussian 16*, Revision B.01, Gaussian, Inc., Wallingford CT, 2016.

(31) (a) Zhao, Y.; Truhlar, D. The M06 Suite of Density Functionals for Main Group Thermochemistry, Thermochemical Kinetics, Noncovalent Interactions, Excited States, and Transition Elements: Two New Functionals and Systematic Testing of Four M06-class Functionals and 12 Other Functionals. *Theor. Chem. Acc.* **2008,** *120*, 215–241. (b) Zhao, Y.; Truhlar, D. G. Density Functionals with Broad Applicability in Chemistry. *Acc. Chem. Res.* **2008,** *41*, 157–167.

(32) Pracht, P.; Bohle, F.; Grimme, S. Automated Exploration of the Low-Energy Chemical Space with Fast Quantum Chemical Methods. *Phys. Chem. Chem. Phys.* **2020**, *22*, 7169–7192. (d) Grimme, S. Exploration of Chemical Compound, Conformer, and Reaction Space with Meta-Dynamics Simulations Based on Tight-Binding Quantum Chemical Calculations. *J. Chem. Theory Comput.* **2019**, *15*, 2847–2862.

(33) Scalmani, G.; Frisch, M. J. Continuous Surface Charge Polarizable Continuum Models of Solvation. I. General Formalism. *J. Chem. Phys.* **2010**, *132*, 114110.

(34) Friestad, G. K.; Mathies, A. K. Effects of α-Alkoxy Substitution and Conformational Constraints on 6-*exo* Radical Cyclizations of Hydrazones via Reversible Thiyl and Stannyl Additions. *Tetrahedron* **2007**, *63*, 9373–9381.

(35) Petrassi, H. M.; Sharpless, K. B.; Kelly, J. W. The Copper-Mediated Cross-Coupling of Arylboronic Acids and *N*-Hydroxyphthalimide at Room Temperature: Synthesis of Aryloxyamines. *Org. Lett.* **2001**, *3*, 139–142.

(36) Feng, X.-H.; Zhang, G.-Z.; Chen, C.-Q.; Yang, M.-Y.; Xu, X.-Y.; Huang, G.-S. Copper(II) Acetate–Mediated Cross-Coupling of Phenylboronic Acids with Aryloximes: Synthesis of O-Aryloximes. *Synth. Commun.* **2009**, *39*, 1768–1780.

(37) Paderes, M. C.; Keister, J. B.; Chemler, S. R. Mechanistic Analysis and Optimization of the Copper-Catalyzed Enantioselective Intramolecular Alkene Aminooxygenation. *J. Org. Chem.* **2013**, *78*, 506–515.

(38) Fernandes, R. A.; Gangani, A. J.; Panja, A. Synthesis of 5-Vinyl-2-isoxazolines by Palladium-Catalyzed Intramolecular *O*-Allylation of Ketoximes. *Org. Lett.* **2021**, *23*, 6227–6231.

(39) Darmency, V.; Scanlan, E. M.; Schaffner, A. P.; Renaud, P. Radical Allylation of *B*-Alkylcatecholboranes. *Org. Synth.* **2005**, *83*, 24–30.

(40) Zhdankin, V. V.; Kuehl, C. J.; Krasutsky, A. P.; Bolz, J. T.; Simonsen, A. J. 1-(Organosulfonyloxy)-3(1*H*)-1,2-benziodoxoles: Preparation and Reactions with Alkynyltrimethylsilanes. *J. Org. Chem.* **1996**, *61*, 6547–6551.

(41) Li, N.; Sun, B.; Liu, S.; Zhao, J.; Zhang, Q. Highly Enantioselective Construction of Dihydrooxazines via Pd-Catalyzed Asymmetric Carboetherification. *Org. Lett.* **2020**, *22*, 190–193.